Effects of Optical Attenuation and Consumption of a Photobleaching Initiator on Local Initiation Rates in Photopolymerizations

Guillermo Terrones*

Process Science and Engineering Department, Pacific Northwest National Laboratory, P.O. Box 999, Richland, Washington 99352

Arne J. Pearlstein*

Department of Mechanical and Industrial Engineering, University of Illinois at Urbana−Champaign, 1206 West Green Street, Urbana, Illinois 61801

Received July 17, 2000; Revised Manuscript Received February 5, 2001

ABSTRACT: For free-radical photopolymerization with a photobleaching initiator, we develop an unsteady one-dimensional model accounting for initiator consumption and optical attenuation and derive relationships for the spatial and temporal variation of the local initiator concentration and initiation rate. With increasing absorbance, the local initiation rate becomes increasingly nonuniform and assumes the form of a highly localized traveling wave propagating with speed $\phi I_0/C_{A,0}$ (where ϕ, I_0, and $C_{A,0}$ are the quantum yield of photoinitiator consumption, incident intensity, and initial photoinitiator concentration, respectively), independent of photoinitiator absorption coefficient. At high attenuation, the maximum photoinitiation rate (as a function of position) is asymptotically one-fourth the initial rate at the front of the layer. Qualitative effects of nonuniform initiation in free-radical photopolymerizations with simple and more complicated kinetics are discussed in terms of the model and results.

Introduction

Photopolymerization is central to many processes, including rapid prototyping of solid objects by stereolithography, dental applications, tape casting, formation of electrophoresis gels, photocuring of adhesives, photolithography, and in situ fabrication of hydrogels for drug delivery and postsurgical sealing and adhesion prevention. Material performance is frequently sensitive to spatial variation in the degree of cross-linking or other sources of structural heterogeneity (e.g., pools of unreacted monomer).[1−8] Predicting and controlling spatial variation of properties in photopolymerized materials therefore requires detailed understanding of the spatiotemporal variation of kinetic processes, including light absorption, chain initiation, propagation, and termination, and cross-linking.

An important characteristic of photochemical reactions, including photopolymerizations, is nonuniformity of the reaction rate, due to dependence of local rates on local light intensity.[9] At any instant, the local light intensity is necessarily a function of position, since light must be absorbed along the path of propagation if reaction is to occur. Rates of primary photochemical processes (e.g., radical formation by initiator photolysis) are generally proportional to the product of concentration and local light intensity and will thus be nonuniform. Moreover, in most photopolymerizations, photoinitiator is photobleached by conversion to moieties transparent or having lower absorption coefficients at the actinic wavelength. Since, at each wavelength, light intensity I decreases along the beam direction x according to the integrated form of Beer's law

$$I(x,t) = I_0 \exp\left[-\sum_{i=1}^{N} \alpha_i \int_0^x C_i(x',t)\, dx'\right] \qquad (1)$$

reduction of the magnitude of the argument of the exponential as reaction progresses will lead to temporal increase of light intensity at each point, corresponding to greater penetration. Here, $I(x,t)$ is the light intensity within the medium, I_0 is the incident light intensity at the optical entrance, and α_i and C_i are the wavelength-dependent absorption coefficient[10] and concentration of the ith absorbing species, of which there are N. Optical attenuation necessarily gives rise to spatial and temporal variation in the local rates of photochemical processes and subsequent kinetic steps. The importance of these effects increases with increasing initiator concentration.

Photopolymerization at high initiator concentration is attractive for two reasons. As initiator concentration increases, spatially averaged polymerization rates typically increase, pass through a maximum, and then decrease due to attenuation.[11−13] Moreover, deleterious effects of volume shrinkage, such as low final monomer conversion, are reduced at high initiator concentrations,[8,14] since monomer conversion is faster than shrinkage at high polymerization rates.

Experimentally, the contribution of attenuation to spatial variation in photopolymerization kinetics has been identified in dental applications,[3−7,15] including in situ restoration of caries and fabrication of dentures and elastomeric impressions of teeth and oral mucosal surfaces. Depth-resolved hardness measurements of photopolymerized dental materials show a strong dependence on photoinitiator concentration and incident light intensity. Since these materials are normally used in thick section, the depth of cure is important, especially in in situ restoration or removable prostheses, due to potentially toxic in-service monomer elution.[15−17] Increased incidence of retention failure, leakage, and caries, compared to nonphotochemically polymerized restorations, have also been linked to inadequate depth of cure.[1]

Proper choice of photoinitiator concentration and incident light intensity is important in other high-absorbance photopolymerization processes. In a photo-

* To whom correspondence should be directed.

10.1021/ma001235y CCC: $20.00
Published on Web 04/14/2001

polymerization that produces polyacrylamide electrophoresis gels with elastic properties superior to those produced by other means, Lyubimova et al.[18] have shown that the gel-point time depends sensitively on photosensitizer concentration, light intensity, and layer thickness. An approximate theory[19] accounts for the time dependence of the photosensitizer concentration but not its spatial variation, which is likely to be important given the significant initial absorbances of ~0.6 and 2.6 in 2 and 10 mm layers, respectively.[18] Attenuation and kinetic effects have also been recently discussed in the context of photopolymerization-induced phase separations.[20]

Experimental studies have quantitatively assessed effects of photoinitiator concentration and light intensity on overall rates and final conversion of monomer. Ruyter,[2] Cook,[5,6] and Cook and Standish[7] have discussed effects of exposure time, light intensity, attenuation, and inhibitor and photosensitizer concentrations on depth of cure. Cook[3] proposed a "lumped" (ordinary differential equation in time) model to approximately account for spatial nonuniformity in depth-of-cure and heat transfer predictions in photopolymerization of urethane dimethacrylate oligomer systems. His model allows for consumption of inhibitors (e.g., O_2), but not for spatiotemporal variation of photosensitizer/photoinitiator concentration or light intensity.

Nonuniformity due to strong attenuation of incident light is essential in confining reaction to a thin surface layer in layered microstereophotolithographic fabrication of three-dimensional structures by photopolymerization.[21−23] Photobleaching of sensitizer results in increased optical penetration and loss of resolution normal to the surface. The work of Flach and Chartoff[21,22] focuses on understanding lateral nonuniformity in depth of penetration and cure associated with Gaussian variation in incident radiation intensity, as well as temperature variations due to nonuniform absorption and reaction. Bertsch et al.[23] report measurements of the width and depth of the photopolymerized region as a function of incident energy per unit area, where the independent variable is presumably the product of time and incident light intensity, neither of which is given separately. The measured depth is in qualitative agreement with the predictions of a model that assumes that (a) partial photobleaching occurs and (b) complete polymerization occurs at a point as soon as the "threshold energy per volume" of "1 J cm^{-1}" at that point is exceeded. (Note that the threshold value cited has units inconsistent with both its definition and eq 5 of ref 23.)

More generally, Mateo et al.[24] discussed how nonuniformity of the photoinitiation rate can affect the molecular weight distribution, which like other quantities not predicted by simple kinetic models, can be expected to depend on whether account is taken of attenuation and initiator consumption. For "unstirred" systems (i.e., with no mass transfer), Shultz and Joshi[25] present expressions for the spatial variation of the *initial* photopolymerization rate. For this case, they presented no results at later times (when nonhomogeneous consumption of photoinitiator will be important) for either the spatial variation of the photoinitiation rate or the average photopolymerization rate.

Goodner and Bowman[8] recently considered a one-dimensional unsteady photopolymerization model that accounts for attenuation and photoinitiator consumption and incorporates a kinetic scheme allowing for diffusion-limited propagation and termination at high degrees of monomer conversion. They studied polymerization of 3 mm layers of 2-hydroxyethyl methacrylate at two concentrations of an initiator (2,2-dimethoxy-2-phenylacetophenone; DMPA) for which the absorbance of the layer is unchanged during the course of the reaction, and for one concentration of a hypothetical initiator which has the same absorption coefficient as DMPA, but undergoes complete photobleaching. Contour plots of photopolymerization rate (with one additional plot of fractional conversion of monomer) showed clear evidence of nonuniformity at high initiator concentrations.

Although the importance of attenuation in photopolymerization kinetics has been clear for some time,[11,26] the standard theoretical treatment[26,27] is flawed in two respects.

First, it does not account for spatial variation of the initiation rate. Within its assumptions (no diffusion, monochromatic illumination, quasi-steady state), the standard model begins, correctly, with an expression for the local steady-state free-radical polymerization rate (in terms of moles per unit volume per unit time)

$$R_p = k_p[M]\sqrt{R_i/(2k_t)} \tag{2}$$

where k_p and k_t are the propagation and termination rate constants, respectively, [M] is the monomer concentration, and R_i is the (local) initiation rate, represented by

$$R_i = 2\phi I_a \tag{3}$$

Here, I_a is the volumetric photon absorption rate, measured in einsteins per unit volume per unit time, and ϕ is the quantum yield of consumption of initiator in

$$A \xrightarrow{h\nu} 2R^{\bullet} \tag{4}$$

It is then asserted that I_a is given by $I_0(1 - e^{-\epsilon[A]b})$,[28] where I_0 is the "incident light intensity", i.e., the photon flux (einsteins per unit area per unit time), ϵ is the initiator "molar absorptivity (extinction coefficient)", [A] is the initiator concentration, and b is described as the thickness of the reacting system or distance into the reaction vessel. (A summary of the variables used is provided in Table 1).

In fact, if the photoinitiator concentration did not change with time, the local volumetric photon absorption rate would be properly given by

$$I_a = \alpha[A]I_0e^{-\alpha[A]x} \tag{5}$$

(ref 9, eq 6−107). Expressions[26,27] of the form $I_0(1 - e^{-\epsilon[A]b})$ correspond to the integral, over the layer thickness, of the volumetric photon absorption rate. If the initiator concentration is uniform and steady, one can use eqs 2, 3, and 5 to obtain an expression for the local polymerization rate

$$R_p = k_p[M]\sqrt{\phi\alpha[A]I_0e^{-\alpha[A]x}/k_t} \tag{6}$$

The expression given for R_p in eq 3-65 of Odian[26] has dimensions inconsistent with those for the same symbol used elsewhere in that work. Incorrect expressions given by Mateo et al.[24] for R_p are dimensionally inconsistent with each other (cf. their eqs 1 and 2 and their eqs 2 and 3).

Table 1

symbol	quantity	definition	units
b	layer depth or position in layer		m
C	concentration		M
I	light intensity		einsteins m^{-2} s^{-1}
I_a	volumetric photon absorption rate		einsteins m^{-3} s^{-1}
I_0	incident light intensity		einsteins m^{-2} s^{-1}
I_v	volumetric photon absorption rate		einsteins m^{-3} s^{-1}
k_p	propagation rate constant		M^{-1} s^{-1}
k_t	termination rate constant		M^{-1} s^{-1}
L	layer depth		m
R_i	initiation rate		einsteins m^{-3} s^{-1}
$\tilde{R}_i$	dimensionless initiation rate	$R_i/(\phi I_0 \alpha_A C_{A,0})$	
R_p	polymerization rate		M s^{-1}
S	dimensionless concentration	$C_A/C_{A,0}$	
$\bar{S}$	mean dimensionless concentration		
t_{diff}	characteristic diffusion time	L^2/D	s
x	dimensional coordinate		m
y	dimensionless coordinate	$\alpha_A C_{A,0} x$	
z	dimensionless coordinate	x/L	
α	absorption coefficient		M^{-1} m^{-1}
γ	initial absorbance	$\alpha_A C_{A,0} L$	
ϵ	extinction coefficient		M^{-1} m^{-1}
τ	dimensionless time	$\phi I_0 \alpha_A t$	
ϕ	quantum yield of initiator consumption		

Related issues are raised in the development of a model to predict photoinitiator consumption rates.[14] The authors cite Odian[29] in asserting (their eq 1) that the rate of decrease of photoinitiator concentration is equal to $I_v(1 - e^{-\epsilon[A]b})$, where I_v, ϵ, and b are the "light intensity in units of energy per unit volume", "initiator extinction coefficient", and "reaction vessel thickness", respectively. First, dimensional consistency requires that I_v has dimensions of energy per unit volume *per unit time* and is therefore a *volumetric photon absorption rate* (einsteins per unit volume per unit time) rather than an "intensity" (einsteins per unit area per unit time). Second, since it accounts for attenuation but allows no spatial variation, the authors' eq 1 must pertain to the rate of decrease of the *spatially averaged* initiator concentration. That rate is equal to the product of the quantum yield of the initiation reaction (4) and the (spatially averaged) volumetric absorption rate $I_0 \cdot (1 - e^{-\alpha[A]b})/b$, rather than the expression $I_v(1 - e^{-\epsilon[A]b})$ cited above. (The work of Lissi and Zanocco[12] correctly predicts spatially averaged photopolymerization rates for systems in which the initiator concentration is steady and uniform.)

The primary consequence of these limitations is that the results are applicable to a very restricted class of systems. When attenuation is important enough to be accounted for in computing the local light intensity or spatially averaged initiation rate, neglecting the spatial variation of initiator concentration restricts use of computed initiation rates to systems that are well-mixed (e.g., by stirring or buoyancy-driven convection[30,31]) or those with very small absorbance

$$\sum_{i=1}^{N} \epsilon_i \int_0^L C_i(x,t)\, dx \qquad (7)$$

Neither the standard treatment,[26,27] its variants,[14,15,24] nor (6) accounts for spatial and temporal variation in initiator concentration accompanying reaction. When absorbance decreases due to photobleaching of initiator,[11,32] this leads to reduced attenuation and nonuniformity as the reaction progresses, an advantage recognized by Goodner and Bowman.[8]

We are aware of no experimental data for the spatial or temporal variation of initiation rates, kinetics, monomer conversion, or initiator consumption in photopolymerizations, although the issues have been recognized. In a study of camphorquinone-initiated photopolymerization of several dimethacrylates, Cook[33] stated that "data influenced by CQ depletion (which is most likely to occur under conditions of high conversion and radiation intensity) was excluded from the analysis." Similarly, Sastre et al.[34] remark, in an investigation of photopolymerization of lauryl acrylate initiated by *N*-acetyl-4-nitro-1-naphthylamine and *N*,*N*-dimethylaniline, that "In order to avoid having to make a correction for the effect of initiator depletion on the reaction rates observed, lower incident light intensities were used in subsequent experiments so that the per cent of initiator depletion as a function of irradiation time could be neglected." Neglecting data taken under conditions where initiator consumption is significant has the effect of limiting the range of applicability of any rate law derived therefrom.

In what follows, we develop general relationships for spatiotemporal concentration variation of a photobleaching initiator in systems where attenuation and initiator consumption are accounted for and use them to compute local initiation rates. This work complements that of Goodner and Bowman[8] in that it focuses on the spatiotemporal variation of the initiation rate, which is relatively independent of the kinetic model appropriate to a particular free-radical photopolymerization, and can be used as an "input" to a variety of detailed kinetic schemes. Use of the results in polymerization models with simple and complex kinetics is then discussed.

Model

In developing a model in which attenuation and photoinitiator consumption compete to determine the local initiator concentration and light intensity distribution, and hence the local initiation rate, we restrict attention to a single-step reaction with first-order kinetics (4).

We consider a one-dimensional unsteady model in a layer of thickness L subject to uniform illumination normal to the surface at $z = 0$, as shown in Figure 1. If

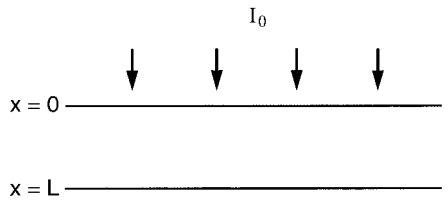

Figure 1. Definition sketch.

the initiator A undergoes only photochemical reaction, the variation of its concentration C_A is governed by

$$\frac{\partial C_A}{\partial t} = -\phi\alpha_A I(x,t)\, C_A(x,t) \tag{8}$$

where α_A is the absorption coefficient of A, and transmission and absorption of light are assumed to be described by Beer's law (1). When only A absorbs, the variation of initiator concentration along the optical path satisfies

$$\frac{\partial C_A}{\partial t} = -\phi\alpha_A I_0 \exp\left[-\alpha_A \int_0^x C_A(x',t)\, dx'\right] C_A \tag{9a}$$

We assume that the reactant concentration is initially uniform throughout the layer, so that

$$C_A(x,0) = C_{A,0} \tag{9b}$$

Equation 9a explicitly excludes mixing due to flow, such as thermally driven buoyant convection that sometimes occurs in photopolymerizations,[30,31] or diffusion. Convective transport in photopolymerization and other photochemically reacting systems can sometimes be prevented or inhibited by choice of the direction of illumination,[35] conducting the process in a polymer gel or high-viscosity medium,[36] fluid rotation,[37] or by reducing the gravitational acceleration.[38−40]

The number of parameters upon which the solution of (9a,b) depends is reduced by defining dimensionless independent and dependent variables $\tau = \phi I_0 \alpha_A t$, $z = x/L$, and $S = C_A/C_{A,0}$, along with the dimensionless parameter $\gamma = \alpha_A C_{A,0} L$, which is proportional to the initial absorbance. With this nondimensionalization, (9a,b) can be written as

$$\frac{\partial S}{\partial \tau} = -\exp\left[-\gamma \int_0^z S(z',\tau)\, dz'\right] S \tag{10a}$$

subject to the initial condition

$$S(z,0) = 1 \tag{10b}$$

Equations 10a and 10b constitute an initial value problem for a nonlinear integro-differential equation.

The mean of the dimensionless concentration over the thickness of the layer

$$\bar{S}(\tau) = \int_0^1 S(z,\tau)\, dz \tag{11}$$

satisfies an ordinary differential equation

$$\frac{d\bar{S}}{d\tau} = -\frac{1}{\gamma}(1 - e^{-\gamma\bar{S}}) \tag{12a}$$

obtained by integrating (10a) over $0 \le z \le 1$, subject to

$$\bar{S}(0) = 1 \tag{12b}$$

The solution of (12a,b) is

$$\bar{S}(\tau) = \frac{1}{\gamma} \ln[1 - (1 - e^{\gamma})e^{-\tau}] \tag{13}$$

The exact solution of (9a,b) can be written in terms of our dimensionless variables as

$$S(z,\tau) = [1 - e^{-\gamma z}(1 - e^{\tau})]^{-1} \tag{14}$$

a result derived by several authors since the work of Wegscheider.[41]

We note that for a semiinfinite layer, for which $L \to \infty$, we can define a new dimensionless coordinate, $y = \gamma z$, in terms of which we can write

$$S_\infty(y,\tau) = [1 - e^{-y}(1 - e^{\tau})]^{-1} \tag{15}$$

In this case, no mean dimensionless concentration $\bar{S}$ can be defined.

Results

We present results for the photoinitiator concentration distribution and local photoinitiation rate, covering the entire range of behavior from small values of the initial absorbance $\gamma = \alpha_A C_{A,0} L$, where attenuation and nonuniformity are negligible, up to large values of γ, for which light absorption and reaction are highly localized.

Photoinitiator Concentration Distributions. We begin by presenting dimensionless concentration profiles (as functions of $z = x/L$) of the photoinitiator concentration for several values of the dimensionless parameter γ, at fractional initiator consumptions $1 - \bar{S}$ of 0.1, 0.25, 0.5, 0.75, and 0.9. We note that (14) can be written in terms of $\bar{S}$ according to

$$S(z,\bar{S}) = \frac{1 - e^{-\gamma\bar{S}}}{1 - e^{-\gamma\bar{S}} + e^{\gamma(1-\bar{S}-z)} - e^{-\gamma z}} \tag{16}$$

so that for any value of $\bar{S}$, the photoinitiator concentration profile depends only on γ. At any fractional consumption, the maximum and minimum values of S occur at $z = 1$ and 0, respectively. We define their difference by $\Delta(\bar{S}) = S(1,\bar{S}) - S(0,\bar{S})$, which provides a measure of the degree of inhomogeneity in the initiator concentration across the layer. By differentiation, it is easy to show that the maximum value of Δ is attained when $\bar{S} = 1/2$ and that

$$\Delta_{max} = \Delta(1/2) = \tanh(\gamma/4) \tag{17}$$

Thus, the maximum concentration difference between the front and rear of the layer approaches zero as $\gamma \to 0$, while in the limit of large γ, $\Delta_{max} \to 1$, corresponding to nearly complete consumption of initiator at $z = 0$ before significant consumption occurs at the rear of the layer.

For $\gamma = 0.1$, Figure 2a shows that the profiles are almost uniform, due to the fact that for small values of γ, the third and fourth terms in the denominator of (16) are practically constant, thus suppressing the source of nonuniformity.

For $\gamma = 1$, Figure 2b shows profiles of the photoinitiator concentration for the same values of $\bar{S}$. The initiator profiles are nearly linear over the entire layer, with a definite nonzero slope. The concentration differ-

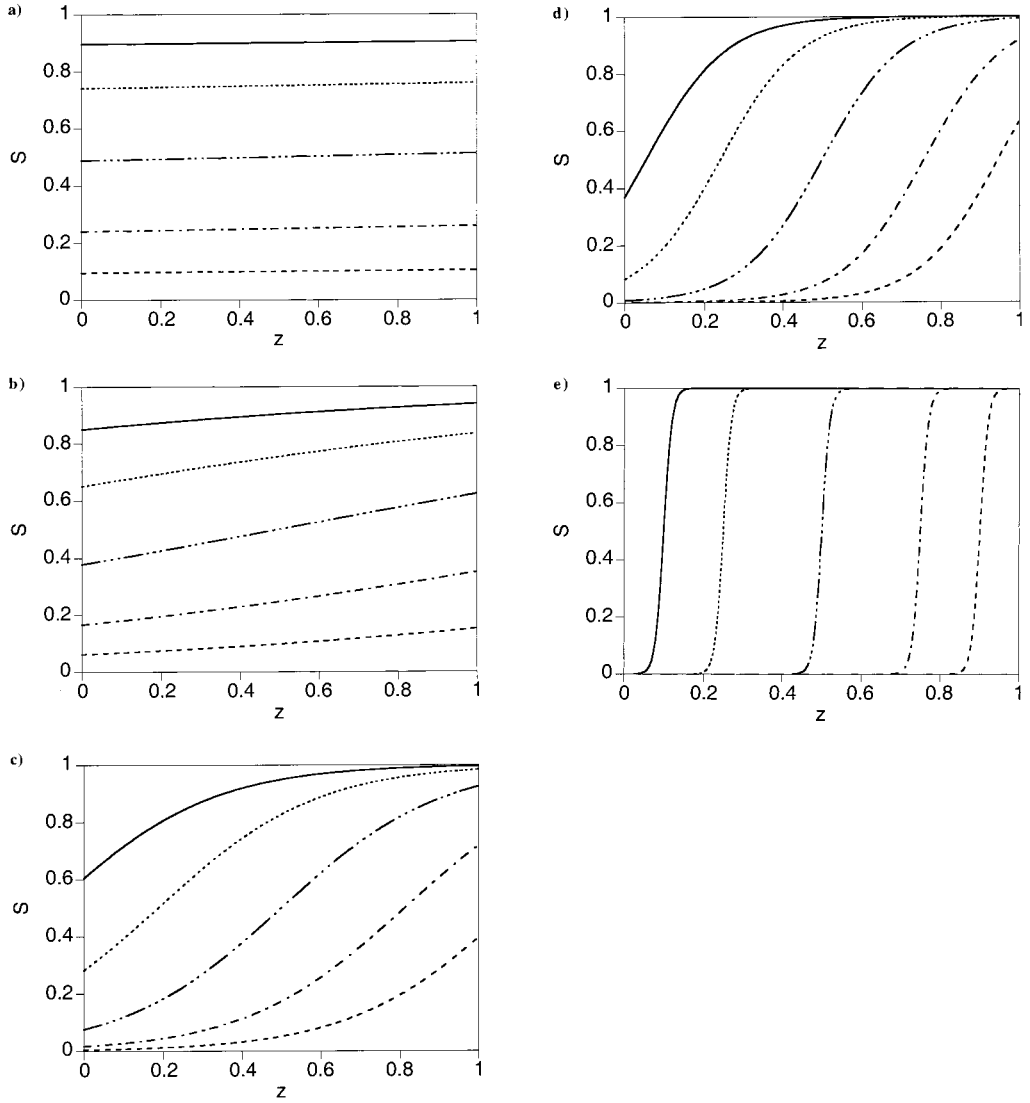

Figure 2. Dimensionless photoinitiator concentration profiles $S = C_A/C_{A,0}$ as functions of $z = x/L$ at different degrees of photoinitiator consumption $1 - \bar{S}$: —, $\bar{S} = 0.9$; ···, $\bar{S} = 0.75$; — ··· —, $\bar{S} = 0.5$; — · —, $\bar{S} = 0.25$; - - -, $\bar{S} = 0.1$. (a) $\gamma = 0.1$, (b) $\gamma = 1$, (c) $\gamma = 5$, (d) $\gamma = 10$, and (e) $\gamma = 100$.

ence across the layer reaches its maximum at a fractional consumption of 50%, as predicted by (17).

Figure 2c shows that for $\gamma = 5$ the curvature of the concentration distributions becomes prominent. At low fractional consumptions, most of the reaction has occurred near the optical entrance, and relatively little photoinitiator has been consumed elsewhere. As the degree of initiator consumption increases, more light penetrates through to each position in the layer, and the initiator consumption rate away from the optical entrance increases. Near the end of the process, very little of the remaining initiator is near $z = 0$.

For $\gamma = 10$, Figure 2d shows photoinitiator distributions that are even more nonuniform. No significant reaction of initiator has occurred in the rear half of the layer by the time 25% of the initiator has been consumed. By 50% consumption, little initiator remains in the front half of the layer, while little has been consumed in the rear half.

For $\gamma = 100$, Figure 2e shows that the photoinitiator concentration profile has a large gradient at some position for each value of $\bar{S}$. The sequence of profiles is similar to that of a traveling wave, which is the form that the solution approaches as $\gamma \to \infty$. The speed of the wave can be estimated by taking S to be constant (say $S = S^*$) in (14), solving for and differentiating z with respect to τ at this fixed concentration,[42] and eliminating τ in favor of $\bar{S}$. We obtain

$$\left(\frac{dz}{d\tau}\right)_{S^*} = \frac{1}{\gamma(1 - e^{-\tau})} = \frac{1 - e^{-\gamma}}{\gamma(1 - e^{-\gamma(1-\bar{S})})} \qquad (18)$$

For large γ, (18) predicts that the dimensionless propagation speed is essentially independent of $\bar{S}$ after an initial transient. In that case, since (18) is true for each concentration S^*, it is clear that at large initial absorbances the waveform propagates without change following an initial transient. Thus, for large γ, the dimensionless wave speed is $1/\gamma$, which corresponds to the dimensional wave speed

$$\frac{dx}{dt} = \phi I_0/C_{A,0} \qquad (19)$$

If the initial absorbance is sufficiently high for the right-hand side of (18) to be approximated accurately by $1/\gamma$, the dimensional wave speed will be independent of absorption coefficient.

Since for large γ the photoinitiator concentration is very small upbeam of this front, and the light intensity is very small downbeam, initiation at each value of $\bar{S}$ is strongly localized in a narrow region where the product of the light intensity and initiator concentration is not small. This localization is discussed in more detail in the following subsection.

Photoinitiation Rates. The local photoinitiation rate R_i is given by the negative of twice the right-hand side of (9a), the initiator consumption rate. We can define a dimensionless initiation rate $\tilde{R}_i$

$$\tilde{R}_i = \frac{R_i}{\phi I_0 \alpha_A C_{A,0}} = -2\frac{\partial S}{\partial \tau} = \frac{2e^{\tau-\gamma z}}{[1 - e^{-\gamma z}(1 - e^{\tau})]^2} \quad (20a)$$

from which we can obtain

$$\tilde{R}_i(z,\bar{S}) = \frac{2(e^{\gamma \bar{S}} - 1)e^{-\gamma z}(e^{\gamma} - 1)}{[e^{\gamma \bar{S}} - 1 + e^{-\gamma z}(e^{\gamma} - e^{\gamma \bar{S}})]^2} \quad (20b)$$

(In what follows, we parametrize the extent of reaction by the mean initiator concentration, $\bar{S}$, rather than the time t or dimensionless time τ. Explicit dependence on τ can be recovered using (13) and on t by further using $\tau = \phi I_0 \alpha_A t$.)

We first observe that when half of the photoinitiator has been consumed, $\tilde{R}_i(z,{}^1/_2)$ is symmetric about the midlayer location $z = {}^1/_2$, where it assumes a maximum value. More generally, we can use (20a) to show that in the range of dimensionless time

$$\ln 2 < \tau < \ln(e^{\gamma} + 1) \quad (21a)$$

or equivalently in the range of dimensionless mean initiator concentration

$$\frac{1}{\gamma}\ln\frac{2}{1 + e^{-\gamma}} < \bar{S} < \frac{1}{\gamma}\ln\frac{1 + e^{\gamma}}{2} \quad (21b)$$

there will be some z in the interior of $0 < z < 1$ for which the initiator consumption rate is a local maximum, given by

$$\tilde{R}_{i,max} = \frac{1}{2(1 - e^{-\tau})} = \frac{1 - e^{-\gamma}}{2(1 - e^{-\gamma(1-\bar{S})})} \quad (22a)$$

or in terms of dimensional parameters

$$R_{i,max} = \frac{\phi I_0 \alpha_A C_{A,0}(1 - e^{-\alpha_A C_{A,0} L})}{2(1 - e^{-\alpha_A C_{A,0} L(1-\bar{S})})} \quad (22b)$$

From (22a), it is apparent that, at large γ, $\tilde{R}_{i,max}$ approaches ${}^1/_2$ after a brief transient. We note that the dimensionless initiator consumption rate at $\tau = 0$ ($\bar{S} = 1$) is $\tilde{R}_i = 2e^{-\gamma z}$, so that $\tilde{R}_i$ at $z = 0$ at the beginning of exposure, as shown in Figure 3b.

The spatially averaged rate over the depth of the layer is

$$\tilde{R}_{i,int} = \int_0^1 \tilde{R}_i(z,\bar{S})\, dz = \frac{2}{\gamma}(1 - e^{-\gamma \bar{S}}) \quad (23a)$$

which in dimensional terms is

$$\tilde{R}_{i,int} = \int_0^1 R_i\, dx = \frac{2\phi I_0(1 - e^{-\alpha_A C_{A,0} L \bar{S}})}{L} \quad (23b)$$

Equation 23b explicitly accounts for photoinitiator consumption through the dependence on the instantaneous mean initiator concentration $\bar{S}$.

For small initial absorbances, we expect the photoinitiation rate to be nearly uniform. That this is the case is apparent in Figure 3a, for $\gamma = 0.1$. At low fractional consumptions, $\tilde{R}_i$ is slightly higher in the front of the layer than in the rear (corresponding to the dominant influence of weak attenuation), while at higher fractional consumptions, $\tilde{R}_i$ is slightly lower in the front (corresponding to the dominant influence of slightly greater initiator depletion near $z = 0$). In the limit of small γ, $\tilde{R}_i \approx 2\bar{S}$, with which the numerical results are in excellent agreement.

As the initial absorbance increases, the distribution of $\tilde{R}_i$ at each value of $\bar{S}$ becomes more nonuniform, as is evident in Figure 3b for $\gamma = 1$. The distributions are approximately linear at all $\bar{S}$, with the slope changing sign near $\bar{S} = {}^1/_2$. An interesting feature is that the rate at the rear of the layer remains nearly constant over the first 50% of the reaction, changing by less than 3%. In fact, during that period, $\tilde{R}_i$ at the optical exit $z = 1$ always exceeds its initial value. (During that time, the rate at the front wall decreases by more than 60%.) The slight increase in $\tilde{R}_i$ at $z = 1$ results from the increase in light intensity at the rear of the layer (due to upbeam initiator consumption) more than compensating for initiator consumption there (see Figure 2b). We note that for $\bar{S} = {}^1/_2$ there is an interior maximum in $\tilde{R}_i$. For $\gamma = 1$, (21b) shows that this occurs only over the limited range $0.380 \le \bar{S} \le 0.620$.

For $\gamma = 2$, the photoinitiation rate profile (Figure 3c) shows increasing curvature, most noticeably at low conversions while the integral in (10a) is still fairly large for a significant range of z.

For $\gamma = 5$, Figure 3d shows that a local maximum in $\tilde{R}_i$ occurs not only near $\bar{S} = {}^1/_2$ but also over a wide range of $\bar{S}$. For $\bar{S} = 0.75$, 0.5, and 0.25, the local photoinitiation rate assumes a maximum value in the interior of the layer, which propagates downbeam as $\bar{S}$ decreases. As predicted by (22a), the maximum rate approaches (from above) ${}^1/_4$ of the $z = 0$ initial rate.

At still higher initial absorbance, spatial distributions of $\tilde{R}_i$ become more complicated. For $\gamma = 10$, Figure 3e shows that the photoinitiation rate becomes spatially nonmonotonic by the time 10% of the photoinitiator has been consumed. According to (21b), this nonmonotonic profile begins at $1 - \bar{S} = 0.069$ and persists until $1 - \bar{S} = 0.931$. This peaked distribution propagates downbeam with relatively little change in form and is nearly symmetric about its maximum. The maximum rate is a bit more than ${}^1/_4$ of the initial value at the front wall, consistent with (22a). The dimensionless half-width at half-maximum $(\Delta z)_{hwhm} = 1.763/\gamma = 0.1763$ can be computed from (20b). (The corresponding dimensional half-width is $(\Delta x)_{hwhm} = 1.763/(\alpha_A C_{A,0})$.) Thus, at any time, $\tilde{R}_i$ is less than ${}^1/_2$ of its maximum value over more than 60% of the layer. This waveform propagates downbeam until the peak exits the layer, at which time $\tilde{R}_i$ decreases rapidly at $z = 1$ and everywhere else in the layer. The wavelike behavior is a clear manifestation of the fact that $\tilde{R}_i$ is equal to the product of initiator concentration and light intensity. At high initial absorbances, the initiator concentration changes rapidly at some position, being low upbeam of that point and high downbeam. Similarly, the light intensity is high upbeam of that point and low downbeam. At each value of $\bar{S}$,

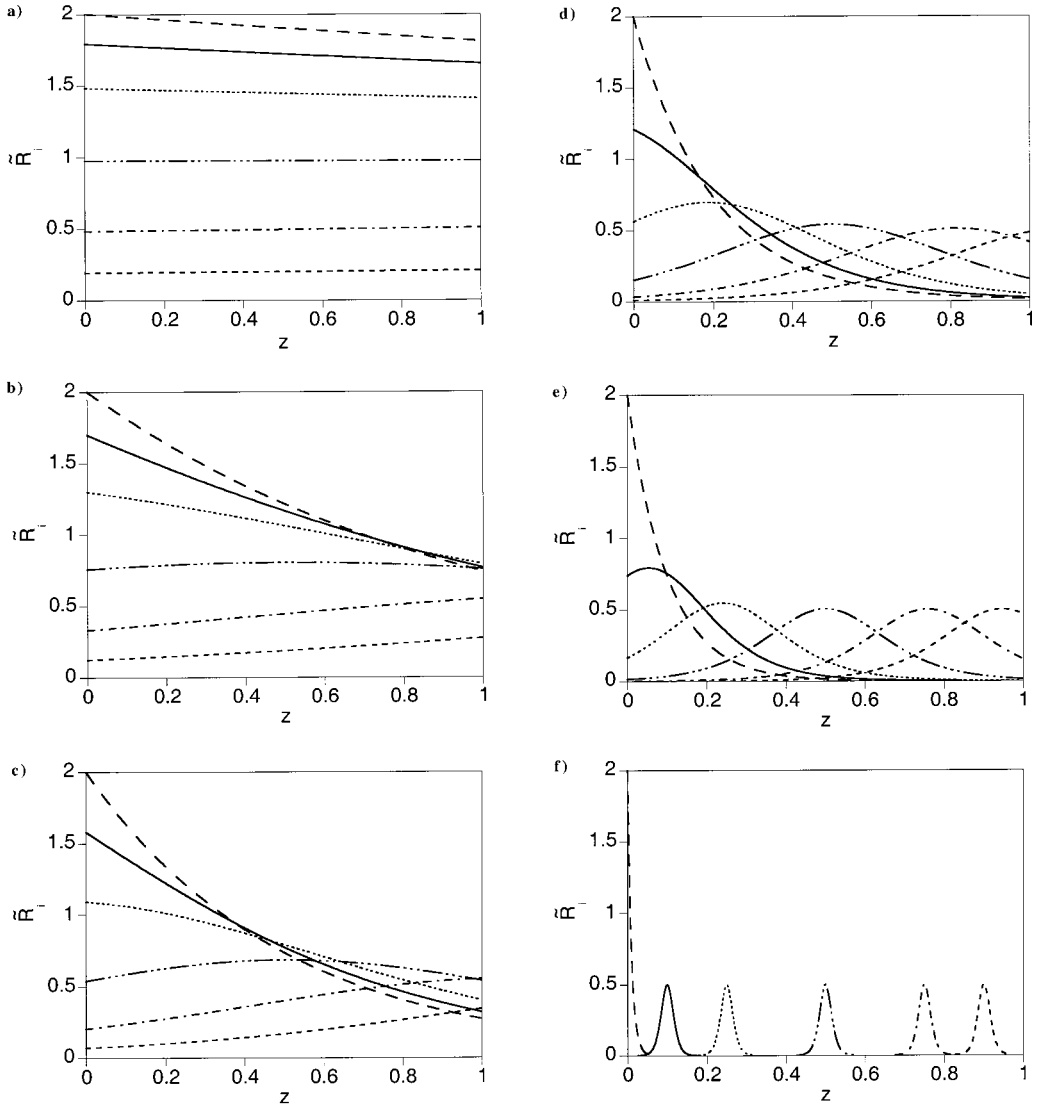

Figure 3. Dimensionless photoinitiation rate profiles $\tilde{R}_i = R_i/(\phi I_0 \alpha_A C_{A,0})$ as functions of $z = x/L$ at different degrees of photoinitiator consumption $1 - \bar{S}$: — — —, $\bar{S} = 1$; —, $\bar{S} = 0.9$; ···, $\bar{S} = 0.75$; — ··· —, $\bar{S} = 0.5$; — · —, $\bar{S} = 0.25$; - - -, $\bar{S} = 0.1$. (a) $\gamma = 0.1$, (b) $\gamma = 1$, (c) $\gamma = 2$, (d) $\gamma = 5$, (e) $\gamma = 10$, and (f) $\gamma = 100$.

their product reaches a maximum near that point, which gives rise to the wavelike behavior described.

For $\gamma = 100$, the spatiotemporal variation of the photoinitiation rate (Figure 3f) is a sharply peaked traveling wave highly localized at the front predicted by (18). The magnitude rapidly approaches $^1/_4$ of the $z = 0$ initial rate. The dimensionless and dimensional half-widths at half-maximum are 1.732×10^{-2} and $1.763/(\alpha_A C_{A,0})$, respectively. Note that for large γ, the wave speed given by (18) is essentially constant after an initial transient, and that according to (13) the overall degree of initiator consumption varies almost linearly with τ. The "photoinitiation zone" moves steadily downbeam as initiator is consumed.

Finally, we note that for complete photobleaching in a semiinfinite layer, Figure 4 of Bertsch et al.[23] shows wavelike behavior of the local volumetric photon absorption rate similar to that shown here for the local photoinitiation rate. Presentation of their results in terms of position and time variables with arbitrary units, and the lack of a closed-form solution (i.e., our eq 15 for the photoinitiator concentration distribution and the analogue

$$\tilde{R}_i = \frac{R_i}{\phi I_0 \alpha_A C_{A,0}} = -2\frac{\partial S}{\partial \tau} = \frac{2e^{\tau - y}}{[1 - e^{-y}(1 - e^{\tau})]^2} \qquad (24)$$

of (20a) for the photoinitiation rate) hinders interpretation and use. From (24), we see that for $\tau \geq \ln 2$ the maximum concentration occurs at $y = \ln(e^{\tau} - 1)$ and that the half-width at half of the maximum rate is $(\Delta y)_{hwhm} = 2.0634$. Comparison to Figure 4 of ref 23 shows that the half-width at half-maximum in that figure is about 8.41 (in "arbitrary units"), and the maximum in the volumetric photon absorption rate at each time shown (also in "arbitrary units") is at a position whose coordinate (in "arbitrary units") is numerically almost equal to the time. Thus, we see that both the depth and time shown there are related to our dimensionless variables $y = \gamma z$ and $\tau = \phi I_0 \alpha_A t$ by multiplying the latter variables by approximately 4.07.

Discussion

The analysis and computations above predict local rates of photoinitiator consumption and photoinitiation as functions of position and time for all values of the light intensity, quantum yield, initial initiator concentration, and absorption coefficient.

A key question is "Under what conditions is nonuniformity unimportant in the context of photopolymerization kinetics?" Clearly, if the initial absorbance is small, then the photoinitiation rate will be essentially uniform throughout the entire layer, and nonuniformity will generally be unimportant regardless of the detailed photopolymerization kinetics. However, as the initial absorbance increases, so will the degree of nonhomogeneity of the initiation rate. An important result above is that when attenuation is strong, the spatiotemporal variation of the initiation rate asymptotically assumes the form of a traveling wave. As a result, essentially the entire layer (except for thin regions at the front and rear, the thicknesses of which vanish as $\gamma \rightarrow \infty$) is ultimately "exposed" to the same "photoinitiation rate history". Since at each location in the layer, the integral from $\tau = 0$ to ∞ of the initiation rate

$$\int_0^\infty \tilde{R}_i(z,\tau)\, d\tau = -2\int_0^\infty \frac{\partial S}{\partial \tau}\, d\tau = -2S(z,\tau)\Big|_0^\infty = 2[S(z,0) - S(z,\infty)] = 2 \quad (25)$$

is constant, the same number of radicals will ultimately be created at each point. However, even if the initiator is consumed throughout the layer before the monomer is fully converted and the polymerization kinetics are adequately described by the steady-state rate law (2) at each point, the degree of monomer conversion will still be nonuniform throughout the layer when the initiator is completely consumed. This is because spatiotemporal variation of initiation rate affects the local primary radical concentration, and hence the radical chain concentrations and termination rates. As a result, other properties, such as molecular weight distribution,[24] may be affected.

In most photopolymerization applications, initiator is not consumed throughout the layer before the monomer reaches its final degree of conversion. Thus, the number of radicals created at each depth is determined by evaluating the integrals in (25) at *finite* upper limits (corresponding to the value of τ at which illumination ends). Since the time integral of the initiation rate is spatially uniform only if the upper limit is infinite (corresponding to complete initiator consumption), the integrated value of $\tilde{R}_i$ will necessarily vary with position. Moreover, if photopolymerization kinetics and characteristics such as molecular weight distribution depend jointly on the histories of the concentrations of monomer and initiator (and possibly an inhibitor[6,7]) and are not fully described by (2), then spatial variation is inevitable. A few examples will serve to illustrate the point. In each case, the computed local photoinitiation rate $\tilde{R}_i$ (or its dimensional counterpart R_i) can be used in an appropriate model of photopolymerization kinetics.

First, if simple steady-state kinetics are appropriate, then one can use $\tilde{R}_i$ in (2) to compute the local photopolymerization rate. Second, if the kinetics at high degrees of monomer conversion are complicated by reduction of either the "quantum yield of initiation"[43] (as opposed to the quantum yield of (4) defined above) or the effective termination or propagation rate constants due to reduced radical mobility,[8,44,45] or by autoacceleration,[46,47] then $\tilde{R}_i$ can be used directly in a more sophisticated kinetic model. Third, if the radical chain length depends on initiation rate,[33] then adequate description of the process will require knowledge of the spatiotemporal variation of $\tilde{R}_i$. Such a dependence can be expected to lead to spatial variation in the radical chain length and molecular weight distribution when attenuation is significant. Finally, spatiotemporal variation of initiation rate will also be important when a free-radical inhibitor such as oxygen is present in the reacting medium[3,15,34] and is nonhomogeneously consumed.[48] In all of these cases, the photopolymerization kinetics will vary from point to point, so that it is important to know the spatiotemporal variation of the photoinitiation rate.

An example of these effects is the wavelike progress of monomer conversion discussed by Goodner and Bowman[8] for a photobleached initiator. This has its origin in the high-absorbance propagation of a photoinitiation wave, with the additional complexity of diffusion-limited propagation and termination kinetics.

A clear experimental manifestation of downbeam photoinitiation wave propagation at high initial absorbance is the depth-of-cure phenomenon. While direct comparison of the asymptotic dimensional photoinitiation front wave speed given by (19) to experimental data[3−5,16] on the time dependence of the depth of cure is precluded by the important role played by O_2 inhibition,[3,15] the expression (20a) for the photoinitiation rate can be used in computations of the spatiotemporal variation of monomer and inhibitor concentrations.

Spatiotemporal variation of photoinitiation rate can have important effects on the kinetic chain length and molecular weight distribution. When the average chain length decreases with increasing initiation rate, locations at which significant (or almost complete) monomer conversion occurs before the maximum initiation rate has reached that location will have higher average molecular weights than upbeam locations at which photopolymerization occurred at higher initiation rates. This effect might be most important at intermediate absorbances (e.g., $1 \leq \gamma \leq 10$; see Figure 3b−e), for which nonuniformity of the initiation rate is significant, but attenuation is not so strong as to localize initiation as a traveling wave at all stages of reaction.

As a consequence, polymer properties that depend on molecular weight distribution will vary along the propagation direction. At high optical attenuation, initiation is highly localized, so that one can in principle use a time-periodic or other time-dependent incident light intensity to control the depth dependence of the molecular weight distribution, degree of cross-linking, etc. Other approaches, including frontal polymerization,[49,50] capable of tailoring property variation normal to a surface, are not suitable for thin layers. Temporal control of light intensity might be useful in building nonuniform hydrogels having prescribed release histories[51] or in optimizing properties of polymer/liquid crystal composites[20,52] and other materials.

Our results have implications for the choice of light intensity and photoinitiator concentrations in cases where optical attenuation is important. If the quantum yield, absorption coefficient, and initial concentration of the initiator are specified, then (19) provides a relationship between the incident intensity and the time required for the photoinitiation wave to reach the rear of the layer. Another example is the situation in which inhibition involves a species (e.g., O_2) that is present in the layer initially and can diffuse into the layer as it is consumed.[41,53,54] In that case, polymerization at a given depth will not occur unless the initiation rate exceeds the rate at which inhibitor diffuses to that depth. Equation 22b allows one to compute the minimum

incident intensity that will achieve a local photoinitiation rate sufficient to consume the inhibitor. For an inhibitor that diffuses in from the front of the layer, the required intensity will decrease as the polymerization front moves rearward, since the rate of inhibitor transport will decrease with distance (and also with the degree of monomer conversion).

There are also situations in which bulk diffusion of photoinitiator or monomer can be important. In layers thin enough for the characteristic diffusion time $t_{diff} = L^2/D$ to be comparable to or less than the characteristic time for reaction, t_{rxn}, diffusion can play a significant role. For a typical photopolymerization time $t_{rxn} = 60$ s and $D = 5 \times 10^{-6}$ cm^2 s^{-1}, this requires $L \leq 170$ μm, the thickness of hydrogels photopolymerized in situ by Hubbell and co-workers to prevent formation of adhesions in postsurgical wound treatment.[55] (By the same criterion, if $D > 9 \times 10^{-7}$ cm^2 s^{-1}, then diffusion will be significant in the 37 μm layers photopolymerized in 15 s by the same group.[56]) Bulk diffusion effects have been accounted for in other high-absorbance multispecies radical-chain photochemical systems with multistep kinetics,[57] but to the best of our knowledge, not in photopolymerizations.

Finally, we note that wave propagation and other spatial variation discussed above can occur in photochemical systems not undergoing polymerization. A recent attempt[36] to verify steady wave propagation in photooxidation of 9,10-diphenylanthracene in a polymer matrix that inhibits convective and diffusive mass transfer showed large departures from predicted wave speeds, which were attributed to poor collimation of the beam.

Conclusion

For a broad class of photoinitiated polymerizations, we have shown how the local initiation rate depends on position and time over the entire range of initial absorbance. For photobleaching initiators under conditions when attenuation is important, initiation propagates downbeam through the layer in the form of a traveling wave, whose speed is determined by the rate of increase of the penetration depth of light. The results demonstrate the importance of accounting for attenuation and photoinitiator consumption effects in photopolymerization modeling. They point the way to incorporation of initiator consumption and nonuniform initiation into models that account for diffusion-limited propagation and termination, autoacceleration, and other kinetic complications and that can predict molecular weight distributions and other properties.

Acknowledgment. The authors thank two anonymous reviewers for bringing Figure 4 of ref 23 and ref 36 to their attention. Pacific Northwest National Laboratory is operated by Battelle for the U.S. Department of Energy under Contract DE-AC06-76RLO 1830. Additional support for this work was provided by NSF Grants MSM-8451157, CTS-9017181, and CTS-9613241.

References and Notes

(1) De Lange, C.; Bausch, J. R.; Davidson, C. L. *J. Oral Rehabil.* **1980**, *7*, 369−377.
(2) Ruyter, I. E. *Acta Odontol. Scand.* **1981**, *39*, 27−32.
(3) Cook, W. D. *J. Appl. Polym. Sci.* **1991**, *42*, 2209−2222.
(4) Hirose, T.; Wakasa, K.; Yamaki, M. *J. Mater. Sci.* **1990**, *25*, 1209−1213.
(5) Cook, W. D. *J. Macromol. Sci., Chem.* **1982**, *A17*, 99−111.
(6) Cook, W. D. *J. Dent. Res.* **1980**, *59*, 800−808.
(7) Cook, W. D.; Standish, P. M. *Aust. Dent. J.* **1983**, *28*, 307−311.
(8) Goodner, M. D.; Bowman, C. N. In *Solvent-Free Polymerizations and Processes. Minimization of Conventional Organic Solvents*; Long, T. E., Hunt, M. O., Eds.; ACS Symposium Series 713; American Chemical Society: Washington, DC, 1998; pp 220−231.
(9) Calvert, J. G.; Pitts, J. N. *Photochemistry*; Wiley: New York, 1966; pp 640−641.
(10) We use the absorption coefficient (ref 9, p 21) for simplicity; it is related to the (decadic) molar absorptivity or extinction coefficient ϵ by $\alpha = \epsilon \ln 10$.
(11) Bengough, W. I.; Ross, I. C. *Trans. Faraday Soc.* **1966**, *62*, 2251−2263.
(12) Lissi, E. A.; Zanocco, A. *J. Polym. Sci., Polym. Chem. Ed.* **1983**, *21*, 2197−2202.
(13) McGinniss, V. D.; Provder, T.; Kuo, C.; Gallopo, A. *Macromolecules* **1978**, *11*, 393−404.
(14) Bowman, C. R.; Peppas, N. A. *Macromolecules* **1991**, *24*, 1914−1918.
(15) Anseth, K. S.; Newman, S. M.; Bowman, C. N. In *Biopolymers II*; Peppas, N. A., Langer, R. S., Eds.; Advances in Polymer Science; Springer: New York, 1995; Vol. 122, pp 177−217.
(16) Lindén, L.-Å. In *Radiation Curing in Polymer Science and Technology*; Fouassier, J. P., Rabek, J. F., Eds.; Elsevier Applied Science: London, 1993; Vol. 4, pp 387−466.
(17) Bland, M. H.; Peppas, N. A. *Biomaterials* **1996**, *17*, 1109−1114.
(18) Lyubimova, T.; Caglio, S.; Gelfi, C.; Righetti, P. G.; Rabilloud, T. *Electrophoresis* **1993**, *14*, 40−50.
(19) Lyubimova, T.; Righetti, P. G. *Electrophoresis* **1993**, *14*, 191−201.
(20) Nwabunma, D.; Kim, K. J.; Lin, Y.; Chien, L. C.; Kyu, T. *Macromolecules* **1998**, *31*, 6806−6812.
(21) Flach, L.; Chartoff, R. P. *Polym. Eng. Sci.* **1995**, *35*, 483−492.
(22) Flach, L.; Chartoff, R. P. *Polym. Eng. Sci.* **1995**, *35*, 493−498.
(23) Bertsch, A.; Jézéquel, J. Y.; André, J. C. *J. Photochem. Photobiol. A: Chem.* **1997**, *107*, 275−281.
(24) Mateo, J. L.; Bosch, P.; Vázquez, E.; Sastre, R. *Makromol. Chem.* **1988**, *189*, 1219−1227.
(25) Shultz, A. R.; Joshi, M. G. *J. Polym. Sci., Polym. Phys. Ed.* **1984**, *22*, 1753−1771.
(26) Odian, G. *Principles of Polymerization*, 3rd ed.; Wiley: New York, 1991.
(27) Oster, G.; Yang, N.-L. *Chem. Rev.* **1968**, *68*, 125−151.
(28) Note[10] that use of *e* rather than 10 as the base of the logarithm requires use of the absorption coefficient α rather than the molar absorptivity/extinction coefficient ϵ. The focus here is on the differences between functional forms and not on the differences between α and ϵ. In the introduction, ϵ is used when reproducing or discussing expressions of previous authors who have used that quantity.
(29) Odian, G. *Principles of Polymerization*, 2nd ed.; Wiley: New York, 1981.
(30) Brulle, Y.; Bouchy, A.; Valance, B.; André, J. C. *J. Photochem. Photobiol. A: Chem.* **1994**, *83*, 29−37.
(31) Frazier, D. O.; Hung, R. J.; Paley, M. S.; Long, Y. T. *J. Cryst. Growth* **1997**, *173*, 172−181.
(32) Costela, A.; García-Moreno, I.; Dabrio, J.; Sastre, R. *J. Polym. Sci., Part A: Polym. Chem.* **1997**, *35*, 3801−3812.
(33) Cook, W. D. *J. Polym. Sci., Part A: Polym. Chem.* **1993**, *31*, 1053−1067.
(34) Sastre, R.; Conde, M.; Mateo, J. L. *J. Photochem. Photobiol. A: Chem.* **1988**, *44*, 111−122.
(35) Pearlstein, A. J. *J. Phys. Chem.* **1985**, *89*, 1054−1058.
(36) Rytov, B. L.; Ivanov, V. B.; Ivanov, V. V.; Ansimov, V. M. *Polymer* **1996**, *37*, 5695−5698.
(37) Nagy, I. P.; Pojman, J. A. *J. Phys. Chem.* **1996**, *100*, 3299−3304.
(38) Sturm, D.; Müller, R.; Rath, H.-J. In *Proceedings of the VIIIth European Symposium on Materials and Fluid Sciences in Microgravity*, ESA SP-333; European Space Agency: Paris, 1992; Vol. 2, pp 895−899.
(39) Avci, D.; Thigpen, K.; Mathias, L. J. *Polym. Prepr.* **1996**, *37* (2), 317−318.
(40) Briskman, V.; Kostarev, K.; Moshev, V.; Guseva, L.; Mashinsky, A.; Nechitailo, G. AIAA Paper 96-0257, 1996.
(41) Wegscheider, R. *Z. Phys. Chem.* **1923**, *103*, 273−306.
(42) Mauser, H. *Z. Naturforsch. B* **1967**, *22*, 569−573.

(43) Kurdikar, D. L.; Peppas, N. A. *Macromolecules* **1994**, *27*, 4084−4092.
(44) Tryson, G. R.; Shultz, A. R. *J. Polym. Sci., Polym. Phys. Ed.* **1979**, *17*, 2059−2075.
(45) Goodner, M. B.; Bowman, C. N. *Macromolecules* **1999**, *32*, 6552−6559.
(46) Bowden, M. J. In *Macromolecules. An Introduction to Polymer Science*; Bovey, F. A., Winslow, F. H., Eds.; Academic: New York, 1979; pp 43−44.
(47) Muggli, D. S.; Burkoth, A. K.; Keyser, S. A.; Lee, H. R.; Anseth, K. S. *Macromolecules* **1998**, *31*, 4120−4125.
(48) Müller, U. *J. Macromol. Sci., Pure Appl. Chem.* **1996**, *A33*, 33−52.
(49) Pojman, J. A.; Ilyashenko, V. M.; Khan, A. M. *J. Chem. Soc., Faraday Trans.* **1996**, *92*, 2825−2837.
(50) Epstein, I. R.; Pojman, J. A. *An Introduction to Nonlinear Chemical Dynamics: Oscillations, Waves, Patterns, and Chaos*; Oxford: New York, 1998.
(51) Lu, X.; Anseth, K. S. *J. Controlled Release* **1999**, *57*, 291−300.
(52) Wang, X. Y.; Yu, Y.-K.; Taylor, P. L. *J. Appl. Phys.* **1996**, *80*, 3285−3290.
(53) Smith, D. K. *Photogr. Sci. Eng.* **1968**, *12*, 263−266.
(54) Pappas, S. P. In *Radiation Curing. Science and Technology*; Pappas, S. P., Ed.; Plenum: New York, 1992; pp 1−20.
(55) Hill-West, J. L.; Dunn, R. C.; Hubbell, J. A. *J. Surgical Res.* **1995**, *59*, 759−765.
(56) Hill-West, J. L.; Chowdhury, S. M.; Slepian, M. J.; Hubbell, J. A. *Proc. Natl. Acad. Sci. U.S.A.* **1994**, *91*, 5967−5971.
(57) Terrones, G.; Pearlstein, A. J. *J. Am. Chem. Soc.* **1991**, *113*, 2132−2140.

MA001235Y